GLULAM FRAMES ADHESIVELY BONDED BY MEANS OF BIRCH PLYWOOD PLATES: PRELIMINARY INVESTIGATIONS

Tianxiang Wang[1], Yue Wang[2], Roberto Crocetti[3], Magnus Wålinder[4], Pontus Persson[5], Patrik Hedlund[6]

ABSTRACT: The design of timber connections is of great importance since their performance is decisive for timber structures. The widely adopted technique utilizing the slotted-in steel plates could possibly be replaced by using timber-based gusset plates due to the significant advantages in terms of the environmental impact, economy, ease of prefabrication, and fire resistance of the latter one. Among the timber-based panels, plywood made of birch was chosen in the study due to the combined benefits of the cross laminated configuration of plywood and the superior mechanical properties of birch compared to most softwoods. In this paper, a preliminary experimental investigation was carried out to study the structural performance of the glulam trusses connected by means of bonded birch plywood gusset plates. Tests were performed on ad-hoc designed frame-like specimens. The plywood gusset plates were under-designed to be the weakest link in the structure, so as to study their load-bearing capacity. The knowledge obtained in this study is the first step towards the establishment of a model for the design of truss nodes with bonded plywood gusset plates. In the study, the face grain orientation of birch plywood was varied (0°, 5°, and 15° to the horizontal axis) in three test series. Test results show that the influence of the face grain angle from 0 to 15 degrees on the global stiffness of the frame structure is insignificant and it can be well predicted by a simplified planar 2D numerical models. Two analytical models, namely, the classic so-called 'Whitmore model' along with a more accurate analytical model, were utilized to illustrate the failure mechanism of birch plywood gusset plates with the concept of the effective width and the spreading angle.

KEYWORDS: Glue connection, Birch plywood, Glulam frame, Face grain angle, Effective width, Spreading angle

1 INTRODUCTION

Timber, as a building material, is paid more attention in the field of civil engineering, due to its low carbon footprint and lightweight. The design of timber connections is of great significance since their performance is decisive for timber structures. In high-rise timber buildings as well as long-span timber applications, slotted-in steel plates are widely used in joints [1]. Nevertheless, plywood plates could be an alternative to slotted-in steel plates. Timber-based gusset plates are more environmental-friendly and cost-effective, with less prefabrication demand and better fire resistance.

Essentially, two types of connections, namely connections with mechanical fasteners and bonded connections, can be adopted between plywood and other timber elements. Bonded connections are generally stronger, stiffer, and cheaper than mechanical connections. However, bonded connections have more severe requirements during assembly, e.g., the surrounding environment, applied pressure, curing time, etc., [2].

Bonded connections between plywood and other timber elements have been studied for a long time. Crutis [3]

performed a number of tests on rigid lumber frames in 1960. Douglas fir plywood plates were nailed and glued to the Douglas fir lumber framing members. Three types of failures were summarized: (1) stud or rafter failed due to combined bending and axial load, (2) gusset plates failed due to combined bending and axial load, and (3) gusset plates failed in rolling shear. The effect of the face grain angle of plywood gusset plates was also investigated. It was indicated that the orientation of the face grain has a significant effect on the joint capacities. Wilkinson [4] and Josefsson and Larsson [5] compared different connection systems of the structural applications using (1) nailed plywood plate, (2) nailed steel plate, and (3) nailed and glued plywood plate. Their studies found that the third one with nailed and glued plywood plates delivered the highest stiffness and capacities for the structure.

Although connections using plywood gusset plates seem competitive, slotted-in steel plates are still dominant in the marketplace [6]. One reason of that, is the fact that there are still uncertainties - mainly due to lack of experimental data - concerning the load-bearing capacity of plywood under off-axis loading. The load-bearing capacity of the

---

[1] Tianxiang Wang, KTH Royal Institute of Technology, Sweden, tiawan@kth.se
[2] Yue Wang, KTH Royal Institute of Technology, Sweden, yue4@kth.se
[3] Roberto Crocetti, KTH Royal Institute of Technology, Sweden, crocetti@kth.se
[4] Magnus Wålinder, KTH Royal Institute of Technology, Sweden, magnus.walinder@byv.kth.se

[5] Pontus Persson, Kvarteret Konstruktörer, Sweden, pontus.persson@kvarteretk.se
[6] Patrik Hedlund, KTH Royal Institute of Technology, Sweden, phedlu@kth.se

steel plates used in timber connections is, on the other hand, easy to calculate by means of well-proven models. Studies on the structural behavior of birch plywood gusset plates in connections with mechanical fasteners have been initiated recently [7]. This paper aims to gain more knowledge regarding the failure mechanism of bonded birch plywood plates in truss structures. For this purpose, frame-like specimens consisting of glulam elements and laterally bonded birch plywood gusset plates were laboratory tested. Plywood made of birch (*Betula pendula*) was chosen as the material for the gusset plates. The choice of birch is both because it is a wood specie widely available in Scandinavia [8,9] and because it has outstanding mechanical properties. The failure mechanism of the birch plywood plates with varying face grain angles was studied both experimentally and numerically.

2 MATERIALS AND METHODS

2.1 DESCRIPTIONS OF STRUCTURES AND MATERIALS

The structure presented in Figure 1 is composed of inclined members, horizontal members, and birch plywood plates. Inclined and horizontal members made of spruce (Picea abies) glulam GL 28cs were adhesively connected by means of birch plywood gusset plates. Inclined members have an angle of 30° to the horizontal members. The width (direction 1 in Figure 1) and the height (direction 2 in Figure 1) of the frame structure are approximately 1536 mm and 760 mm, respectively. There are three plywood plates at the top and bottom, connected with inclined members, creating four glue lines, annotated as 'Birch plywood A'. Only one gusset plate was glued to the glulam elements on the left and right sides of the frame, connecting the inclined and horizontal glulam elements. This gusset plate, annotated as 'Birch plywood B', was designed to be the weakest link in this structure. Thus, failure in birch plywood B was expected after the destructive test, which is in line with the aim of this paper. The detailed configuration of both birch plywood A and B is shown in Figure 1. The face grain of birch plywood A is parallel to direction 1, while the face grain angle of birch plywood B is varied to investigate its effect on the global behavior of the frame.

All the glulam elements have the same cross-section of 56 mm × 110 mm. These elements were produced from a number of 4 m-long glulam beams GL28cs with a cross-section of 56 mm × 225 mm by using a miter saw and format saw. The weight was measured on each element before the test in order to deduce the density. The mean density was 463 kg/m^3 with a standard deviation (STDV) of 17 kg/m^3. Moisture content (MC) was measured on each glulam element prior to the test by a resistance-based moisture meter (HT 85, GANN, Germany). The mean MC was determined to be 12.6% with a STDV of 1.1%. Five samples were measured by using both HT 85 moisture meter and oven-drying methods [10]. No significant difference between these two methods was observed on glulam elements at a 95% confidence interval. Hence, MC measured from this resistance-based measuring device is considered valid.

Birch plywood plates have a nominal thickness of 9 mm consisting of 7 veneers. The mean density was 714 kg/m^3 (STDV=29 kg/m^3). MC was measured on ten samples cut from the frame specimens after the tests using the oven-drying method. The mean MC was 8.4% (STDV=0.4%). Melamine-urea-formaldehyde (MUF) adhesive (Prefere 4546/5022) was chosen for the tests. The liquid melamine urea adhesive (Prefere 4546) and the liquid hardener (Prefere 5022) were mixed with 100:10 parts-by-weight (pbw). This adhesive system fulfills the requirements according to EN 301 [11] and is classified as a general purpose, gap-filling, and finger-jointing adhesive. However, the applicability of this type of adhesive in this case, i.e., surface bonding between spruce glulam and birch plywood for connection purposes is still uncertain. Therefore, choosing the proper adhesive and the related parameters during assembly is also one of the crucial parts of the investigation for this type of bonded connection.
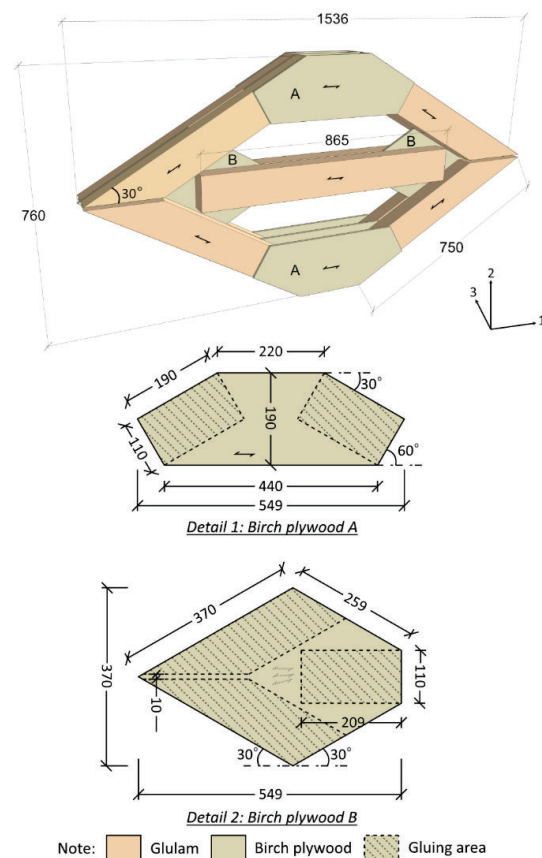

Figure 1: Configuration of the studied frame (Length unit: mm).

2.2 ASSEMBLY PROCESS

The assembly process is illustrated in Figure 2. Firstly, the glued areas were sanded by a sanding machine. The adhesive was spread on both surfaces of birch plywood plates and glulam elements. As shown in Figure 2(b), glulam elements were predrilled with 4 mm holes about 2 cm deep. Clamps were utilized to tighten plywood plates

1454

and glulam together for inserting screws. Two screws with an outer diameter of 3.5 mm and a length of 50 mm were inserted into each glulam element. Then, clamps were removed so that new adhesive layers could be applied (Figure 2(c)). Similar to the previous processes, both glulam element and plywood plates were sanded, spread with adhesive, and pressed by screws (Figure 2(d)). By repeating the aforementioned procedures, all the timber elements were assembled as a whole. Lastly, screws with an outer diameter of 5.6 mm and a length of 140 mm were inserted. The positions of these screws are displayed in Figure 2(e), which are along the center axis of the inclined and horizontal members. It is noted that screws utilized in the frame are only considered for assembly purposes. The influence of the screw on the load-bearing capacity of the joints can be neglected because of their significantly lower shear stiffness, as compared to the shear stiffness of the adhesive.
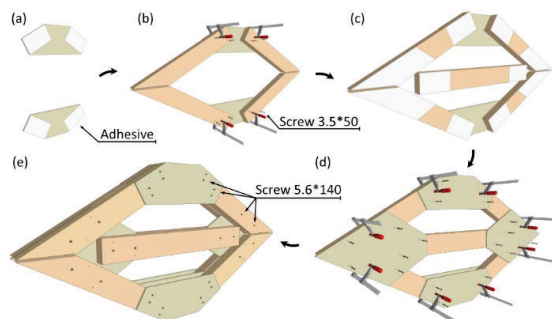

Figure 2: Assembly process of the studied frame.

The adhesive spreading mass per square meter was roughly 400 g/m². The assembled frames were cured for around 1-2 weeks before testing. The indoor temperature during bonding of the specimens was in the range 10-15 °C.

2.3 TEST PROCEDURE

Three test series were performed in the presented study. As displayed in Figure 3(a), the face grain of birch plywood plate B was varied. In test series 1, three frame specimens were tested with the face grain direction of birch plywood B parallel to the horizontal axis. In test series 2 and 3, the face grain angle of birch plywood B was 5° and 15° to the horizontal axis, respectively, with four repetitions.

The test setup is shown in Figure 3(b). Tests were conducted on the MTS810 universal testing machine. All specimens were loaded in compression. During the tests, the loading head motion was constant, with a rate of 1 mm/min. The load signal and the piston movement were recorded simultaneously. In order to avoid applying load directly on birch plywood plates, wedges made of glulam were inserted between the inclined members and birch plywood plates A. The load-bearing capacity was defined as the maximum load attained during the tests. Machine compliance was measured by pressing the loading head to the support, and then it was excluded from the piston movement to derive the vertical displacement of the

frame. The stiffness of the tested structure was defined as the slope of the load-vertical displacement curve in the linear portion.
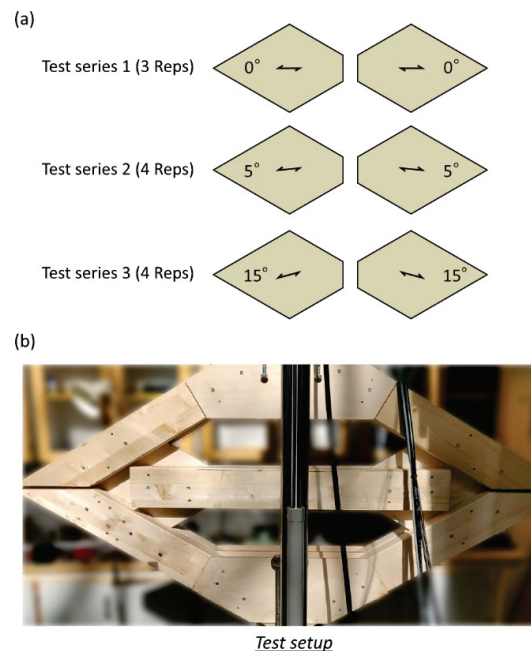
Figure 3: Test series and setup.

2.4 NUMERICAL ANALYSIS

Numerical analyses were performed with commercial finite element software Abaqus (Simulia, USA). A planar 2D numerical model was developed to investigate the structural behavior of the studied frame in the linear elastic stage. Both the stiffness on the global level and the section forces on the component level were checked when the face grain orientation of birch plywood plate B changed from 0° to 5° and 15°.

Ideally, structures of this type can be analyzed as 2D trusses with hinges at each joint [12]. Yet in this study, as can be seen in Figure 1-3, glue connections were adopted, and the proportion of the gluing area to the size of the frame is relatively large. Hence, all the glulam components were modeled as beam-type elements.

Glue-laminated timber is usually characterized as an orthotropic material. It can be further simplified to be transversally isotropic, with identical elastic properties in the radial and tangential directions [13]. The physical and elastic mechanical properties of glulam beam GL28cs assigned in the numerical model are listed in Table 1. The properties include the density ρ, the elastic modulus E_{ij}, the Poisson's ratios ν_{ij}, and the shear modulus G_{ij} (i, j = 1,2,3). Axis 1 is along the grain direction, while axes 2 and 3 are in the transversal directions.

Table 1: *Physical and elastic mechanical properties of glulam GL28cs assigned for numerical analyses.*

ρ (kg/m³)	E_{11} (MPa)	E_{22} (MPa)	E_{33} (MPa)	ν_{12}
463	12500	300	300	0.219

ν_{13}	ν_{23}	G_{12} (MPa)	G_{13} (MPa)	G_{23} (MPa)
0.219	0.582	650	650	65

The input density in Table 1 is the mean value measured in this study and reported in Section 2.1. The elastic properties have been derived according to [14] for the mean values of the elastic modulus and shear modulus and [15] for the Poisson's ratios. Further, the rolling shear modulus G_{23} was assumed to be one-tenth of the shear modulus G_{12} and G_{13} according to [16].

The inclined glulam elements were tied together. For the connection between the inclined and horizontal glulam elements, a spring with the axial stiffness defined in the horizontal direction was assigned in the numerical model. This is due to the fact that there is only one birch plywood plate transferring the axial forces and the potential bending moment between the inclined and horizontal glulam elements. Moreover, the thickness of this plywood plate was under-designed so as to study its failure mechanism after the tests. Therefore, the contribution of this single gusset plate to the global stiffness should be taken into account. It is noticed in Figure 4 that the marked triangular area would take most of the tensile force from the horizontal glulam beams considering that the frame structure was loaded in compression. This marked area was converted into a rectangular shape with the equivalent area. The axial stiffness of the spring can be calculated according to Equation (1).

$$k = \frac{EA}{L} \qquad (1)$$

where k is the axial stiffness of the spring; E is the elastic modulus of birch plywood; A is the cross-sectional area of the converted rectangular shape; and L is the length of the same region. It is worth mentioning that the elastic modulus of birch plywood is angle-dependent. When the face grain orientation of the plywood plate varied from 0° to 15°, the assigned elastic modulus should also be different. The elastic modulus of birch plywood at 0° has been experimentally characterized in previous studies [8], with a mean value of 9.4 GPa. It is also found that one theoretical model can predict the off-axis (between 0° and 90°) elastic modulus fairly well [8]. By employing this theoretical model, the elastic modulus at 5° and 15° could be predicted, which is 8.6 GPa and 5.2 GPa, respectively. See Equation (2) for the calculated axial stiffness for the three tested angles.

$$k = \begin{cases} 5.7 \times 10^7 \ N/m & (\alpha = 0°) \\ 5.2 \times 10^7 \ N/m & (\alpha = 5°) \\ 3.2 \times 10^7 \ N/m & (\alpha = 15°) \end{cases} \qquad (2)$$

where α is the face grain angle of birch plywood plates B to the horizontal axis.

Moreover, the failure load obtained from the test data was applied in the numerical model to check the internal force of each glulam element at failure, especially the horizontal one that would transfer the tensile force to the birch plywood plate B. The numerical stiffness of the global frame structure was derived as the ratio of the input external load to the corresponding vertical displacement at the top of the frame. It would be further compared with the experimental ones in Section 3.1. Glulam elements were meshed with the beam element type (B21 in ABAQUS/CAE 6.14) and the size of 0.02 m.
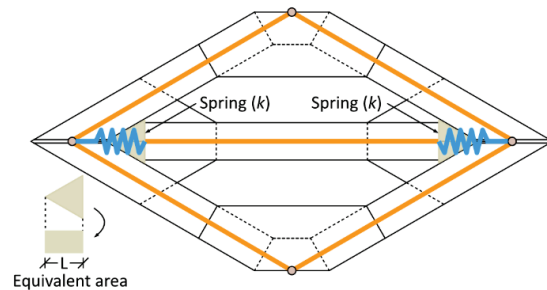
Figure 4: *Illustration of the planar 2D numerical model.*

3 RESULTS AND DISCUSSION

3.1 EXPERIMENTAL RESULTS

The failure load, the stiffness, and the failure mode of each tested frame structure are summarized in Table 2. The experimental load-vertical displacement curves are displayed in Figure 5.

Table 2: *Experimental results*

Test series	Specimen	Failure load (kN)		Stiffness (kN/mm)		Failure mode
01 (0°)	01	72.8		11.2		a
	02	81.1	77.6	9.8	10.5	a
	03	78.8		10.5		a
02 (5°)	01	86.8		10.0		a
	02	81.8	80.6	10.5	10.1	b
	03	74.5		9.7		b
	04	79.3		10.1		a
03 (15°)	01	68.2		8.0		b
	02	76.2	75.2	9.4	8.9	b
	03	79.5		9.0		b
	04	77.0		9.2		b

Note: failure mode 'a' means the bond line failure between birch plywood B and the horizontal glulam while failure mode 'b' represents the failure in birch plywood B.
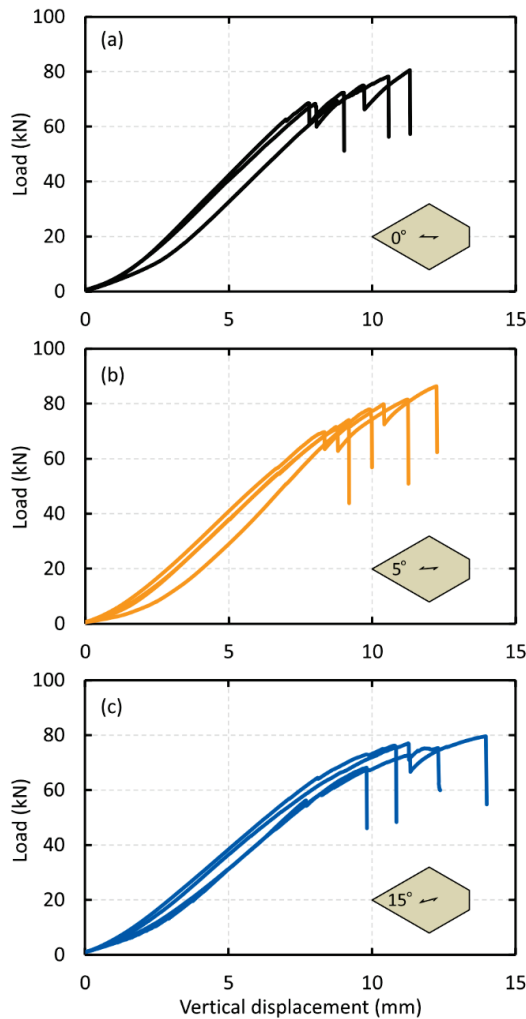
*Figure 5: Experimental load-vertical displacement curves: (a) test series 01 (0°); (b) test series 02 (5°); and (c) test series 03 (15°).*

As noticed in Table 2, test series 02 (5°) has the highest mean failure load, followed by test series 01 (0°) and 03 (15°), which could be explained by the different failure modes. As aforementioned, the birch plywood plate B was designed as the weakest part in the frame. However, for the specimens in the test series 01 (0°), the bond line failure took place prior to the birch plywood failure. The same failure mode was also observed in the first and the fourth specimens in the test series 02 (5°). For the other specimens with the failure occurred in birch plywood, the average failure load of the second and the third specimens in the test series 02 (5°) is 78.2 kN, slightly higher than the average failure load (75.2 kN) of the test series 03 (15°). The stiffness is independent on the failure load and failure mode as it indicates the structural performance in the linear elastic stage. Test series 01 (0°) possesses the highest stiffness, followed by test series 02 (5°) and 03 (15°). It was mentioned in Section 2.4 that the elastic modulus of birch plywood drops rapidly from 9.4 GPa to 5.2 GPa when the face grain angle varies from 0° to 15°

to the loading axis. Nevertheless, the influence of the birch plywood face grain orientation on the global stiffness of the frame is not so dramatic, which can also be observed in Figure 5.

The difference in the load-displacement behavior of each test series is not noticeable, with a slight difference in the failure load and the stiffness as presented in Table 2. All the curves grew slowly in the initial stage, which might be because that the wedges inserted at the top and the bottom of the frame were trying to get full contact with the inclined glulam elements. After this initial consolidation stage, the load increased almost linearly with the vertical displacement in the elastic stage. It is interesting to see that, in some specimens, there was a slight reduction of the load. Then, the load increased again until the final failure of the structure. The slight reduction of the load was owing to the premature 'failure' in a certain part of the bonded area and it was more likely to be seen in the specimens with the final failure also in the bond line. To be more specific, only one specimen in test series 03 showed the load reduction before the final failure (see Figure 5(c)), while in other test series, this phenomenon took place more frequently.

Typical failure modes are presented in Figure 6. As can be seen in Figure 6(a) and Figure 6(b), for the specimens that failed in the bond line, only a small part of glulam failure was observed in the bonded area. It is evident that the strength of the timber material has not been fully exploited, and the bonding quality might have been improved. However, it does not necessarily mean that the MUF adhesives did not work for spruce-birch gluing. In fact, many factors influence the bonding quality, e.g., the surrounding environment (temperature and relative humidity), mixing ratio, assembly time, and pressing methods, etc. It is not a trivial task to determine the influence of each factor on the bonding strength between spruce glulam and birch plywood. Systematic studies should be conducted in the future to propose a proper workflow when manufacturing bonded connections made of birch plywood plates and spruce glulam beams.

Although the bonding quality was not ideal, some specimens showed failure in birch plywood gusset plates (see Figure 6(c) and Figure (d)). The plywood plates failed in tension due to the tensile force transferred from the horizontal glulam beams. The cracks are, in general, perpendicular to the horizontal direction and close to the end of the horizontal glulam beams except for a small part along the face grain direction, as shown in the upper part of Figure 6(c). The axial forces in the glulam elements were not measured during the tests. However, these forces can be estimated with reasonable accuracy by means of a numerical model calibrated with data from experimental results. The failure mechanism of the birch plywood plates can then be discussed with the knowledge of the axial forces reported in Section 3.2 by means of the analytical models proposed in Section 3.3.

(a)

(b)

(c)

(d)
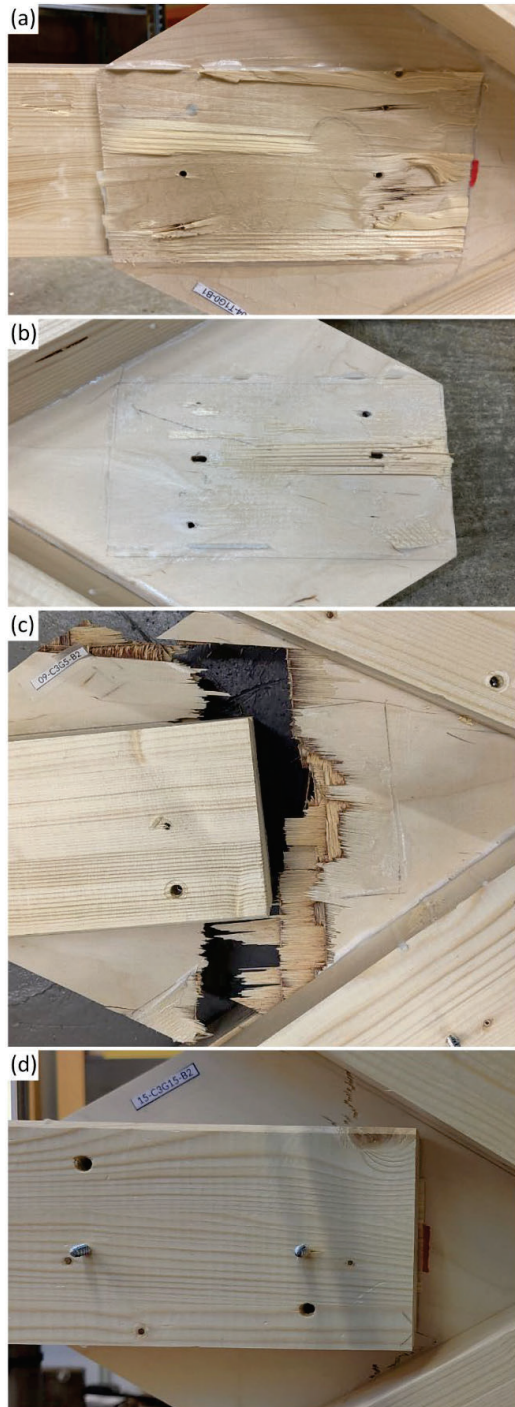
Figure 6: *Typical failure modes: (a) bond line failure in test series 01; (b) bond line failure in test series 02; (c) plywood failure in test series 02; and (d) plywood failure in test series 03.*

Similar studies regarding this frame structure but in mechanical connections have been presented in [7], where the plywood gusset plate B had the face grain orientation parallel to the horizontal axis. Thus, the structural behavior of this timber frame in mechanical connection [7] and glue connection (test series 01 in this study) can

be compared (see Figure 7). Not surprisingly, the adhesively connected one possessed both higher load-bearing capacity and global stiffness.
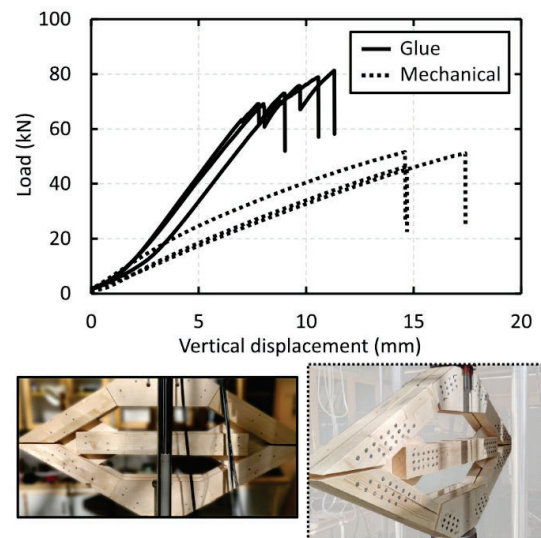
Figure 7: *Load-vertical displacement curves of the frame structures in glue connection (test series 01) and mechanical connection [7].*

3.2 NUMERICAL PREDICTION

Table 3 compares the experimental stiffness with the numerically predicted ones for each test series. The axial forces in the horizontal glulam beams are also listed in Table 3. The underlined numbers indicate that these specimens failed in the bonded area.

Table 3: *Comparison between experimental and numerical results*

| Test series	Specimen	Stiffness (kN/mm)		Axial force in horizontal glulam beams at failure (kN)
		Exp. (Mean)	Num.	
01 (0°)	01	10.5	10.1	81.7
	02			91.0
	03			88.4
02 (5°)	01	10.1	9.9	95.0
	02			89.5
	03			81.5
	04			86.8
03 (15°)	01	8.9	8.0	63.4
	02			70.9
	03			73.9
	04			71.6

The stiffness of the frame structure predicted by the planar 2D numerical model showed good agreement with the experimental results. The numerically predicted stiffness was slightly lower than the experimental stiffness. This might be due to that, in this simplified 2D numerical

model, only the cross sections of glulam elements were defined and the additional thickness of the plywood plates in the glued connection regions was neglected.

Despite the slight difference, this numerical model was considered to be valid and the axial forces in the horizontal glulam beams were checked. The horizontal glulam beams were in tension during loading and the tensile forces were taken by the single birch plywood plate B, leading to the tensile failure of the plywood in some specimens. Two specimens in test series 02 (5°) showed plywood failure. The average tensile force at failure is 85.5 kN. In test series 03 (15°), the average tensile force taken by the plywood plate at failure is lower, which is 70.0 kN.

3.3 ANALYTICAL MODELS

In order to predict the failure load of the gusset plate in timber connections, one design model should be put forward. The first step is to gain knowledge with regard to the strength of the birch plywood plate. In this study, the plywood plates failed in tension with the face grain angle of 5° (in test series 02) and 15° (in test series 03) to the horizontal direction. Hence, the tensile strength of birch plywood at 5° and 15° load-to-face grain angle should be obtained. Wang et al. [8] characterized the off-axis tensile properties of 21 mm birch plywood at around 12% MC and found that the empirical Norris failure criterion predicts the closest results to the experimental data among the investigated linear and quadratic failure criteria (see Figure 8).
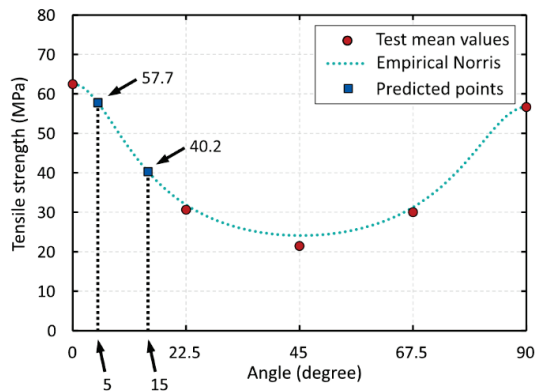
Figure 8: *Tensile strength of birch plywood at any face grain angle to the loading axis predicted by empirical Norris failure criterion.*

It is noticed in Figure 8 that the predicted tensile strength of birch plywood at 5° and 15° are 57.7 MPa and 40.2 MPa, respectively.

Having the tensile force, tensile strength, and the thickness of birch plywood plate at hand, it is possible to derive the width of plywood that was involved in resisting the load, namely, the effective width (see Equation (3)).

$$w_{eff} = \frac{F_t}{f_t \cdot t} = \begin{cases} 164.6\ mm & (\alpha = 5°) \\ 193.5\ mm & (\alpha = 15°) \end{cases} \quad (3)$$

where w_{eff} is the effective width of the birch plywood plate; F_t is the tensile force at failure; f_t is the tensile strength of birch plywood; and t is the plywood thickness. It is evident that the effective width should not be simply assumed as the width of the bonded region, i.e., 110 mm, or the entire crack length, i.e., over 200 mm in Figure 6(c). Besides, the effective width varies at varying load-to-face grain angles. It is worth noting that although the tensile strength of birch plywood decreases roughly 30% when α changes from 5° to 15°, the reduction in the load-bearing capacity of the birch plywood gusset plate in connection is less severe (less than 20%) thanks to the wider w_{eff} at 15°.

The concept of the effective width was first proposed by Whitmore [17] in the last century for the design of the steel gusset plate to mechanically connect other steel members. To define the 'Whitmore effective width' in steel gusset plate, two lines with a spread angle of 30 degrees were drawn from the outer fasteners of the first row to intersect with the line through the bottom row of fasteners. The width between the intersection points is known as the 'Whitmore effective width' [18].

The 'Whitmore effective width' could also be employed in this study for plywood gusset plates in glue connection while the spreading angle should be redefined. See Equation (4) for the derived spreading angle and Figure 9 for the illustration of the adopted 'Whitmore effective width' theory.

$$\theta = \arctan(\frac{w_{eff} - w}{2l}) = \begin{cases} 7.4° & (\alpha = 5°) \\ 11.3° & (\alpha = 15°) \end{cases} \quad (4)$$

where θ is the spreading angle for birch plywood gusset plate; w is the width of the boned area (110 mm); and l is the length of the bonded area (209 mm).
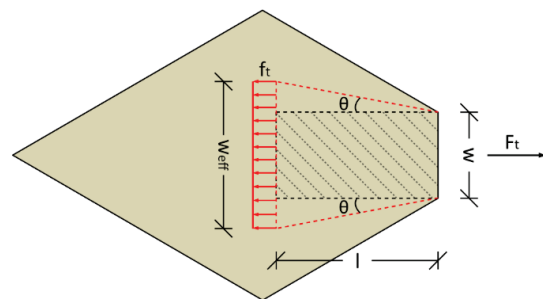
Figure 9: *Illustration of the adopted 'Whitmore effective width' theory.*

As shown in Figure 9, the spreading angle in this classic analytical model starts from the outmost line of the bonded area, resulting in a uniformly distributed tensile stress within the 'Whitmore effective width'.

A modification of the classic analytical model is proposed in the study with the assumption that the tensile force is evenly taken by each part of the bonded area. The bonded area in Figure 10(a) with a width of w and a length of dx could take the tensile force ΔF_t and the tensile stress $\Delta\sigma$ as expressed in Equation (5-7).
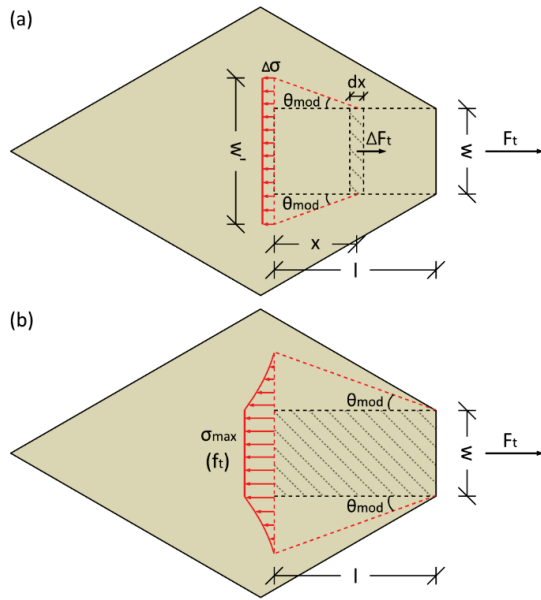
Figure 10: *Illustration of the modified analytical model: (a) the contribution from a calculated bonded region; and (b) the stress distribution.*

$$\Delta F_t = \frac{F_t}{l} dx \tag{5}$$

$$\Delta \sigma = \frac{\Delta F_t}{w' \cdot t} \tag{6}$$

$$w' = w + 2 \tan(\theta_{mod}) \cdot x \tag{7}$$

where θ_{mod} is the spreading angle in the modified analytical model; x is the distance of the calculated bonded region to the end of the bonded area; and w' is the effective width of this calculated region. The effective width of the calculated bonded region decreases when it moves from the outmost to the end of the bonded area, leading to a more realistic non-uniform stress distribution. The maximum tensile stress takes place within the width of the bonded area and can be calculated by performing the integral in Equation (8).

$$\sigma_{max} = \int \Delta \sigma = \frac{F_t}{l \cdot t} \int_0^l \frac{dx}{w + 2 \tan(\theta_{mod}) \cdot x} \tag{8}$$

By solving Equation (8), σ_{max} is expressed in Equation (9).

$$\sigma_{max} = \frac{F_t(\ln(w + 2\tan(\theta_{mod}) \cdot l) - \ln w)}{2l \cdot t \cdot \tan(\theta_{mod})} \tag{9}$$

Imposing that the failure occurs when the maximum tensile stress reaches the tensile strength of birch plywood:

$$\sigma_{max} = f_t \tag{10}$$

θ_{mod} can be determined (see Equation (11)).

$$\theta_{mod} = \begin{cases} 16.6° & (\alpha = 5°) \\ 25.7° & (\alpha = 15°) \end{cases} \tag{11}$$

4 CONCLUSIONS

In this paper, glulam frames were adhesively connected by means of birch plywood plates and tested monotonically in compression. The face grain of the birch plywood connecting the inclined and horizontal glulam elements was 0°, 5°, and 15° to the horizontal direction in three test series. These plywood gusset plates were designed as the weakest part so as to study their failure mechanism. Nevertheless, some specimens failed in the bonded region with little glulam fiber remaining on the bonded surface. Reasons for the failure in the bonded area have been discussed in the paper; however, more studies regarding the adhesive types and process-related parameters should be conducted in the future to enhance the bonding quality for the formation of a reliable bonded connection between spruce glulam and birch plywood. More than half of the tested specimens showed failure in birch plywood plates as expected. Moreover, a comparison between the adhesively bonded and mechanically connected glulam frames confirms the higher load-bearing capacity and global stiffness of the former one. The main findings with regard to the influence of the birch plywood face grain orientation on the global stiffness and load-bearing capacities are as follows:

Global stiffness: despite the anisotropic elastic properties of the birch plywood plate, the influence of its face grain orientation (0° to 15°) on the global stiffness of the tested frame was limited. The global stiffness was also well predicted by the simplified planar 2D numerical model developed in this paper.

Failure mechanism: for the specimens that failed in birch plywood, tensile failure was observed. With the tensile force of the glulam beams at failure load output from the numerical model and the angle-dependent tensile strength of birch plywood characterized in the previous studies, two analytical models, namely, the classic 'Whitmore' and modified analytical models, were utilized to illustrate the failure mechanism with the concept of the effective width and the spreading angle. It is found that, although the tensile strength of birch plywood at 15° is 30% lower than the one at 5°, the effective width and thus the spreading angle is larger at 15°, leading to the smaller difference in load-bearing capacities, which is beneficial for plywood gusset plates in potential structural applications where they are likely to be subjected to the forces in multiple directions.

The spreading angles derived from these two analytical models were determined from the specific frame structure tested in this study. The magnitude of the spreading angle should be further verified by performing uniaxial tests with a wider range of load-to-face grain angles involved, e.g., from 0 to 45 degrees. Moreover, research questions regarding whether the spreading angle theory is robust for birch plywood with different thicknesses and different bonded areas may also need to be considered in the future.

REFERENCES

[1] R. Crocetti. Large-span timber structures. In *Proceedings of the World Congress on Civil, Structural, and Environmental Engineering*, pages 1-23, 2016.

[2] S. Thelandersson, H. J. Larsen. (Eds.). Timber engineering. John Wiley & Sons, 2003.

[3] J. O. Curtis. Design of nailed and glued plywood gussets for lumber rigid frames. *Bulletin (University of Illinois (Urbana-Champaign campus). Agricultural Experiment Station)*, no. 654, 1960.

[4] T. L. Wilkinson. Longtime performance of trussed rafters with different connection systems. US Department of Agriculture, Forest Service, Forest Products Laboratory, 1984.

[5] A. Josefsson, K. Larsson. Ramkonstruktioner av fanerträ, 1991.

[6] T. Wang, Y. Wang, R. Crocetti, and M. Wålinder. Multiple shear plane timber connections with birch plywood and dowel-type fasteners. In *Proceedings of the 17th Annual Meeting of the Northern European Network for Wood Science and Engineering*, pages 131-133, 2021.

[7] Y. Wang, T. Wang, P. Persson, P. Hedlund, R. Crocetti, and M. Wålinder. Birch plywood as gusset plates in glulam frame via mechanical connectors: A combined experimental and numerical study. *J. Build. Eng.*, 105744, 2022.

[8] T. Wang, Y. Wang, R. Crocetti, and M. Wålinder. In-plane mechanical properties of birch plywood. *Constr. Build. Mater.*,340:127852, 2022.

[9] J. Hynynen, P. Niemistö, A. Viherä-Aarnio, A. Brunner, S. Hein, and P. Velling. Silviculture of birch (Betula pendula Roth and Betula pubescens Ehrh.) in northern Europe. *Forestry*, 83(1):103-119, 2010.

[10] BS EN 322: 1993. Wood-based panels – Determination of moisture content. European Committee for Standardization (CEN), 1993.

[11] SS EN 301: 2017. Adhesives, phenolic and aminoplastic, for load-bearing timber structures - Classification and performance requirements. European Committee for Standardization (CEN), 2017.

[12] Z. Chen, D. Tung, and E. Karacabeyli. (Eds.). Modelling Guide for Timber Structures. FPInnovations, 2022.

[13] J. F. Davalos, J. R. Loferski, S. M. Holzer, and V. Yadama. Transverse isotropy modeling of 3-D glulam timber beams. *J. Mater. Civ. Eng.*, 3(2):125-139, 1991.

[14] R. Crocetti, M. Johansson, H. Johnsson, R. Kliger, A. Mårtensson, B. Norlin, A. Pousette, and S. Thelandersson. Design of Timber Structures. Swedish Wood, 2011.

[15] M. Dorn. Investigations on the Serviceability Limit State of Dowel-type Timber Connections [PhD thesis]. Vienna University of Technology, 2012.

[16] H. J. Larsen, J. Munch-Andersen. (Eds.). CIB-W18 Timber Structures - A review of meetings 1-43, 2011.

[17] R. E. Whitmore. Experimental investigation of stresses in gusset plates [Master's Thesis]. University of Tennessee, 1950.

[18] S. J. Chen, C. C. Chang. Experimental study of low yield point steel gusset plate connections. *Thin-Walled Struct.*, 57:62-69, 2012.